Flexible green perovskite light emitting diodes

Article (Accepted Version)

This article has been accepted for publication in a future issue of this journal, but has not been fully edited. Content may change prior to final publication. Citation information: DOI 10.1109/JEDS.2019.2913765, IEEE Journal of the Electron Devices Society

Flexible Green Perovskite Light Emitting Diodes

Giuseppe Cantarella
Sensing Technologies Lab
University of Bozen
Bozen, Italy
giuseppe.cantarella@unibz.it

Sudhir Kumar
Institute for Chemical and Bioengineering
Swiss Federal Institute of Technology (ETH)
Zurich, Switzerland
sudhir.kumar@chem.ethz.ch

Christian Vogt
Institute for Electronics
Swiss Federal Institute of Technology (ETH)
Zurich, Switzerland
christian@cvogt.ch

Stefan Knobelspies
Institute for Electronics
Swiss Federal Institute of Technology (ETH)
Zurich, Switzerland
stefan.knobelspies@ife.ee.ethz.ch

Alain Takabayashi
Institute for Electronics
Swiss Federal Institute of Technology (ETH)
Zurich, Switzerland
alain.takabayashi@epfl.ch

Jakub Jagielski
Institute for Chemical and Bioengineering
Swiss Federal Institute of Technology (ETH)
Zurich, Switzerland
jakub.jagielski@chem.ethz.ch

Niko Münzenrieder
Sensor Technology Research Centre
University of Sussex
Falmer, United Kingdom
n.s.munzenrieder@sussex.ac.uk

Alwin Daus
Department of Electrical Engineering
Stanford University
Stanford, CA, USA
dausa@stanford.edu

Luisa Petti
Sensing technologies Lab
University of Bozen
Bozen, Italy
luisa.petti@unibz.it

Giovanni A. Salvatore
Institute for Electronics
Swiss Federal Institute of Technology (ETH)
Zurich, Switzerland
gasalvatore1982@gmail.com

Paolo Lugli
Sensing Technologies Lab
University of Bozen
Bozen, Italy
paolo.lugli@unibz.it

Chih-Jen Shih
Institute for Chemical and Bioengineering
Swiss Federal Institute of Technology (ETH)
Zurich, Switzerland
chih-jen.shih@chem.ethz.ch

Gerard Tröster
Institute for Electronics
Swiss Federal Institute of Technology (ETH)
Zurich, Switzerland
troester@ife.ee.ethz.ch

***Abstract*—Flexible perovskite light-emitting diodes (LEDs) have attracted increasing interest to realize ultrathin, light weight, highly conformable and nonfragile vivid displays. Solution-processed lead halide perovskite offers numerous distinctive characteristics such as pure emission color, tunable bandgaps, and low fabrication cost. In this work, green perovskite LEDs (PeLEDs) are fabricated on 50 µm thick polyimide substrates. Using colloidal 2D formamidinium lead bromide perovskite emitter, the PeLEDs show a high current efficiency (η_{CE}) of 5.3 cd A^{-1} with a peak emission at 529 ± 1 nm and a narrow width of 22.8 nm. The resultant green emission shows color saturation > 95%, in the Rec. 2020 standard gamut area. To demonstrate mechanical flexibility, the device functionality is tested by dynamic bending experiments down to 10 mm for up to 5000 cycles, resulting in device lifetime over 36 h in a glove box and a drop of η_{CE} and external quantum efficiency (η_{ext}) as low as 15 % and 18 %, respectively. For the selective activation of multiple PeLEDs, 7 x 7 passive arrays on rigid and flexible substrates are demonstrated. Moreover, preliminary results of active matrices show the compatibility of PeLEDs with oxide-based Thin-Film Transistors (TFTs) for display applications.**

Keywords— Perovskite, Light-Emitting Diodes (LEDs), flexible, bending, pixel array, passive matrix, active matrix

I. Introduction

The field of flexible electronics has attracted substantial interest for new and challenging applications, which require electrical functionality on curvilinear and complex surfaces. Together with wearable electronics [1-3] and health monitoring systems [4], flexible displays are considered as most promising candidates for light-weight, ultra-thin, portable, and nonfragile consumer electronics [5]. This new class of displays calls for high performances, high energy efficiency and long-operational stability, as well as low fabrication cost for mass production. In the past years, numerous types of emitters, such as, organic emitters and chalcogenide quantum dots, have been extensively investigated in light emitting diodes to achieve efficient and color pure flexible displays [6, 7]. However, the conventional

International Flexible Electronics Technology Conference ©2018 IEEE

This article has been accepted for publication in a future issue of this journal, but has not been fully edited. Content may change prior to final publication. Citation information: DOI 10.1109/JEDS.2019.2913765, IEEE Journal of the Electron Devices Society

technologies were not able to realize Rec. 2020 standard green emission because of their broad spectral width and a bathochromic shift in photoluminescence after forming the thin solid films. Recently, colloidal organic-inorganic hybrid perovskites (OIHPs) have emerged as the most promising color-pure emitters in light emitting diodes (LEDs) because of their cost-effective facile synthesis at low temperature and easy scalability. Moreover, they show very narrow emission width, tunable bandgap, and high photoluminescence quantum yield (PLQY) [8, 9]. Although few flexible green perovskite LEDs (PeLEDs) have been demonstrated, color-pure electroluminescence that shows a 95% color saturation in Rec. 2020 standard gamut, has never been achieved by far.

In this work, we demonstrate color-pure green flexible PeLEDs using colloidal two dimensional (2D) formamidinium lead bromide ($FAPbBr_3$) perovskite emitters. The 2D $FAPbBr_3$ shows a solid-state PLQY as high as 94%. The devices,

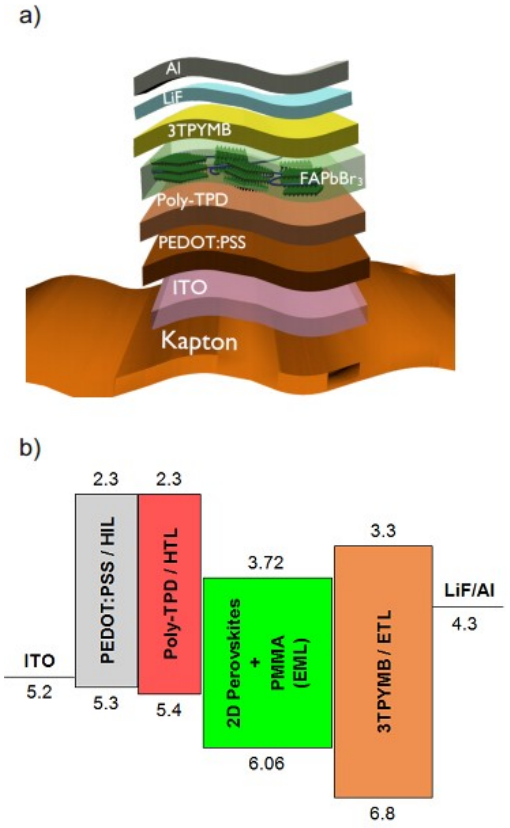

Fig. 1. Perovskite-based LED (PeLED) on flexible substrate. a) Schematic of the device layer stack and b) energy level diagram of materials utilized (data unit: eV).

fabricated on 50 µm thick polyimide foil using a spin-casted emission layer, show a high current efficiency (η_{CE}) of 5.3 cd A^{-1} and a color saturation of ~ 96%. Moreover, the device exhibits a peak emission at 529 nm. Differently from [9], to systematically test the device flexibility under mechanical strain, PeLEDs are evaluated in dynamic bending experiments, showing functionality in a nitrogen-filled glove box down to 10 mm bending radius for up to 5000 bending cycles. Moreover, the fabrication scalability allows the realization of passive and active multi-pixel matrices, consisting of 49 PeLEDs, on both rigid and flexible substrates.

II. MATERIALS AND DEVICE FABRICATION

Monodisperse $FAPbBr_3$ perovskites are synthesized by using the synthetics route reported in ref. [10]. The resultant nanocrystals (NCs) show a PLQYs of ~89% and 94% in solution and spin-casted thin film, respectively. Moreover, the EL emission locate at 531 nm in solution and 529 nm in spin-coated film. The unprecedented higher PLQY in the thin film sample is a result of aggregation induced emission [11]. A schematic architecture of flexible PeLEDs is shown in Fig. 1a. A 50 µm-thick polyimide (Kapton) foil (from DuPont) is utilized as the substrate. First, this substrate is cleaned in acetone and isopropanol for 10 min and cured in oven for 48 h at 200 °C, to remove any solvent residuals. To ensure a high mechanical and chemical stability during the device fabrication, a 50 nm SiN_x, acting as buffer layer, is deposited by PECVD on both sides. Once the Kapton foil preparation is complete, a 120 nm thick ITO anode layer is deposited through RF sputtering in Ar atmosphere. Then, the desirable ITO pattern is obtained through UV photolithography and lift-off process. Subsequently, the patterned ITO substrate is exposed to oxygen plasma for 10 min to ensure a smooth ITO surface without any contamination. Thereafter, a hole injection layer, 32±3 nm PEDOT:PSS, is deposited by spin coating. Then, a hole transporting layer (HTL), 18±2 nm poly[*N,N'*-bis(4-butylphenyl)-*N,N'*-bis(phenyl)-benzidine] (Poly-TPD), is spin-coated in a glovebox. Before spin-coating, colloidal $FAPbBr_3$ NCs are mixed with the low-*k* PMMA host. The resultant emissive layer (30±5 nm) is then deposited onto the Poly-TPD layer. Then, the flexible substrate is transferred to a high vacuum chamber and a 45 nm electron transporting layer, tris(2,4,6-trimethyl-3-(phenyl)borane (3TPYMB), a 1 nm LiF electron injection layer, and a 70 nm Al cathode layer, are sequentially evaporated with the deposition rates of 0.5, 0.1, and ~2 A s^{-1}, respectively. Particularly, the LiF and Al layers are deposited through a shadow mask. The active-area of device is defined as the overlap between ITO and Al layers. Fig. 1b shows the energy band diagram of the materials involved in the device stack.

III. PELEDs ELECTRICAL CHARACTERIZATION

The current density (J) and luminance (L) of a champion device as a function of applied voltage (V) is presented in Fig. 2a. The device shows a low turn-on voltage of 2.8 V and a maximum luminance of 1642 cd m^{-2}. Moreover, our optimized device demonstrate a high η_{CE} of 5.30 cd A^{-1} and a power efficiency (η_{PE}) of 4.76 lm W^{-1} with a high external quantum efficiency (η_{ext}) of 1.29% (see Fig. 2b). As shown in Fig. 2c, PeLEDs exhibit a peak electroluminescence (λ_{EL}) at 529 ± 1 nm and a full width at half maximum of 22.8 nm with Commission internationale de l'éclairage x and y coordinates ($CIE_{x,y}$) of (0.173, 0.768). The $CIE_{x,y}$ color-coordinates presented here show a color saturation of ~96% in the 1931 CIE color space in Rec. 2020 standard gamut area, which has never been achieved in the flexible LEDs so far. We attribute the high device performance to a charge injection balance and efficient recombination of injected carriers under electrical excitation. Moreover, the charge transporting layers, Poly-TPD and 3TPYMB, possessed an efficient carrier (electron and hole)

This article has been accepted for publication in a future issue of this journal, but has not been fully edited. Content may change prior to final publication. Citation information: DOI 10.1109/JEDS.2019.2913765, IEEE Journal of the Electron Devices Society

confinement function. Moreover, our devices also exhibit a consistent EL spectrum with the PL spectra of 2D $FAPbBr_3$ perovskites (Fig. 2c). To the best of our understanding, we present the first flexible PeLED using precise layer controlled colloidal 2D perovskites.

IV. MECHANICAL BENDING EXPERIMENTS

To test the device performance under mechanical stress, a dynamic bending experiment is executed. The flexible substrate, with four PeLEDs (for each device, the emission area is equal to 5 mm x 5 mm) (see Fig. 3a), is mounted on a dynamic bending setup, and bent down to 10 mm bending radius. In this test, the PeLEDs are bent for a certain number of times (100, 500, 1000 and 5000 cycles), and then electrically characterized in ambient condition (see Fig. 3a and 3b), monitoring the η_{CE} and η_{ext}. At zero cycles, the PeLEDs show a η_{CE} and a η_{ext} of 3.47 cd A^{-1} and 0.85%, respectively, at an operational voltage of 3V. Unexpectedly, slightly higher efficiencies are observed after 500 cycles that can be attributed to light induced healing in the perovskite layer. After 5000 cycles, corresponding to > 36 h, the device efficiencies exhibit a drop of 15 % in the η_{CE} and 18 % in the η_{ext} (see Fig. 3c). In general, the lowering of the device performance is mainly attributed to the absence of a passivation layer. Indeed, the interaction with ambient moisture (occurring during the characterization in ambient condition) and the emission layer degradation, is proved by the formation of black lines in the PeLED emitting area (see Fig. 3b). Indeed, future studies need to understand the degradation processes of Perovskites and find possible solutions, to increase device lifetime and broaden the applications of this class of materials [12].

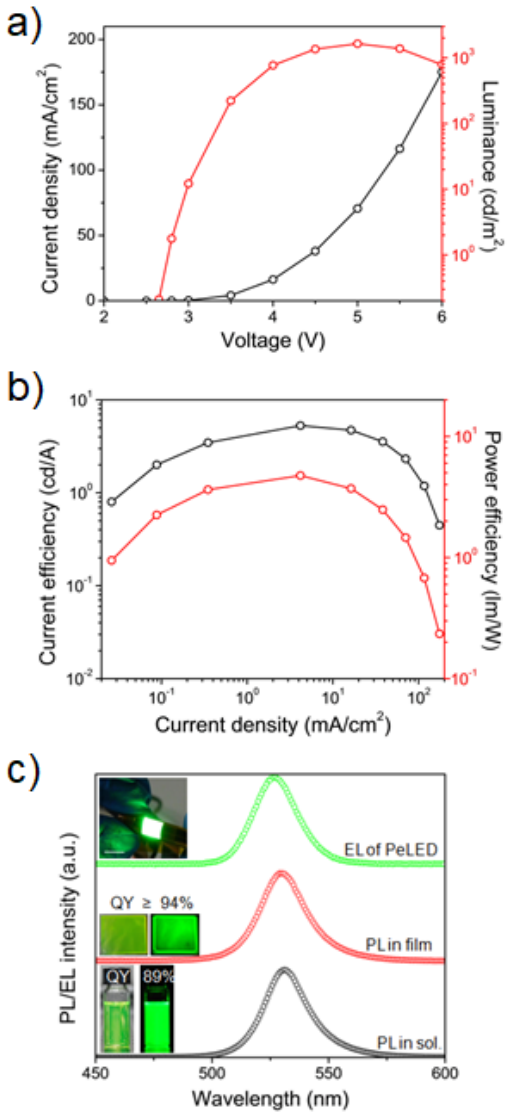

Fig. 2. Flexible PeLED based on 2D $FAPbBr_3$. a) Current density and luminance as a function of voltage. b) Current efficiency and power efficiency as a function of current density. c) Electroluminescence (EL) spectrum at 4 V and photoluminescence (PL) spectra, showing the ultra-pure green emission at 529 ±1 nm. Inset: photograph of flexible PeLED glowing at 4V with a bending radius of 2.5 mm, perovskite thin film on glass substrate (left panel in ambient light and right panel under ultraviolet irradiation), and colloidal solutions of perovskites under ambient light (left panel) and ultraviolet light (right panel).

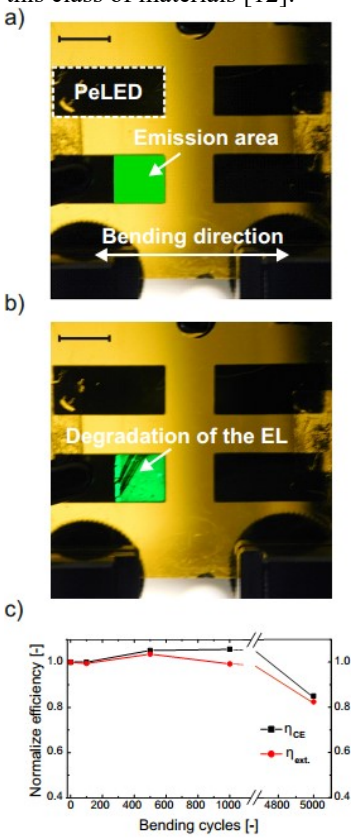

Fig. 3. PeLEDs under dynamic bending experiemnts. a) Optical picture for a) a fresh emitting device (0.5 h lifetime) and b) after 5000 cycles (lifetime > 36 h) (Scale bar: 5 mm). The formation of black lines in the emitting area prove the Perovskite degradation in ambient condition. c) Normalized η_{CE} and η_{ext} for a PeLED bent down to 10 mm bending radius for 100, 500, 1000 and 5000 cycles.

V. PASSIVE MATRIX

The ease of fabrication scalability is demonstrated with the realization of an array of 49 PeLEDs (arranged in 7 lines and 7 columns). The passive matrix consists in a scheme where each

This article has been accepted for publication in a future issue of this journal, but has not been fully edited. Content may change prior to final publication. Citation information: DOI 10.1109/JEDS.2019.2913765, IEEE Journal of the Electron Devices Society

PeLED (or pixel) is activated without any driving circuitry (i.e. capacitors, Thin-Film Transistors (TFTs), etc.). In this way, a pixel is turned on when both its corresponding column line (V_{COL-n}) and row line (V_{ROW-n}) are selected (see Fig. 4a). To prove the fabrication compatibility with flat planes as well as flexible displays, passive PeLED matrices are realized on both glass and Polyethylene terephthalate (PET) substrates, commercially available from Sigma-Aldrich (substrate area = 3 cm x 3 cm). The choice of changing the carriers is due to an higher quality of the ITO layer, acting as anode, with the respect to the sputtered one. Fig. 4b shows the rigid matrix in a custom made setup for the selective characterization of the pixels. In parallel, the flexible array (Fig. 4c) is tested while bending strain is applied, showing functionality down to 1 cm bending radius. A stable EL emission is observed throughout the bending test. Most interestingly, the devices demonstrate stable EL peak at 529 nm during the mechanical strain test.

VI. TOWARDS ACTIVE MATRIX

To prove the compatibility of PeLEDs with other electronics, the next step is their integration with Thin-Film Transistors (TFT), to form an active matrix. For this purpose, metal-oxide semiconductors, and in particular amorphous Indium-Gallium-Zinc-Oxide (a-IGZO), have been widely used for flexible electronics [13-15], due to the low fabrication complexity, large-area deposition and field-effect mobility as high as 10 cm^2/Vs. The active matrix display is designed with an array of 7 x 7 driving cells, where an IGZO TFT drives in series a PeLED, as presented in Fig. 5a. Each single TFT is selected by choosing the corresponding column line V_{COL} and row line V_{ROW}, allowing the PeLED functionality (see Fig. 5a). Considering the J-V curve for the PeLEDs (see Fig. 2a), the W/L ratio for the TFTs is chosen to provide enough drain current I_D. For a LED area of 2 mm x 1 mm and a voltage across the LED of 8.5 V, I_D has to be equal to 2 mA (reached by a W/L = 1400 µm/20 µm) (see Fig. 5b). With these design parameters, the TFTs are fabricated on a flexible 50 µm-thick Polyimide (or kapton) foil using a bottom-gate inverted staggered configuration (see Fig. 5c). Similarly to other works [3], a 120 nm ITO layer is RF sputtered in Ar atmosphere at room temperature, and patterned as the gate contact for the TFT, and anode pad for the PeLED, using a lift-off process in acetone and isopropanol. Afterwards, aluminum oxide (Al_2O_3), IGZO and Ti/Au are deposited as gate dielectric (and passivation layer), semiconductor and source/drain contacts, respectively [16, 17]. To conclude the array fabrication, the TFTs are protected with photoresist (AZ1518, from MicroChemicals) to allow the cleaning of the ITO pads in the PeLED stack by an O_2 plasma treatment, without damaging the TFTs. Once the step is performed, acetone and isopropanol are used to remove the photoresist. Next, the PeLEDs fabrication is performed as presented in paragraph II. An optical picture of the flexible display is presented in Fig. 5c.

The overall matrix uniformity, in terms of electrical properties, is evaluated. The fabrication yield is as high as 96%, with two TFTs (over the whole matrix) not properly functional on the substrate edge, due to damages in the gate dielectric layer, resulting in high leakage current ($I_G > 1$ mA). An average linear mobility μ_{lin}, threshold voltage V_{TH}, subthreshold swing SS and I_{ON}/I_{OFF} ratio of 10.88 cm^2/Vs, 0.86 V, 130 mV/dec and $3.9x10^9$, are extracted. Figure 5d gives an overview of the variation of linear mobility and threshold voltage, while a colored 2D mapping of the same parameters is presented in Fig. 5e and 5f.

Here, additional optimizations are required to improve the active matrix performance, in terms of LED brightness, as well as uniform activation of each pixel. Nevertheless, these preliminary results show the compatibility of oxide-based Thin-Film electronics with Pervoskites, for display applications.

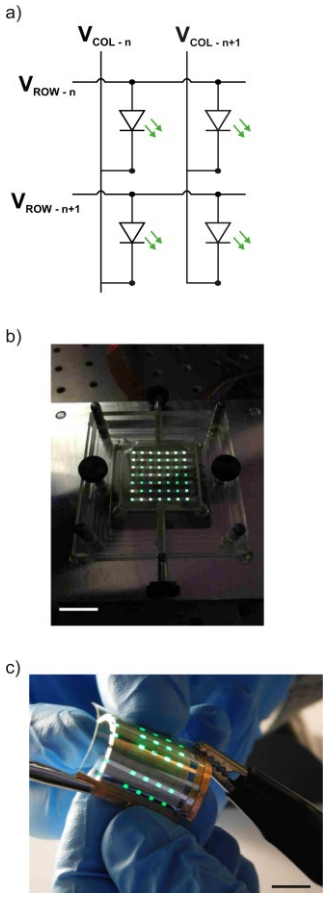

Fig. 4. PeLED passive matrix. a) Layout of a passive matrix, where the selection of a column line (Vcol-n) and a row line (Vrow-n) allows the PeLED activation. An array of 7 x 7 PeLEDs is realized on both b) a rigid glass slide (characterized by using a custom made setup) and (c) on a PET flexible substrate (where Cu tape is used for improving the electrical contact). For both substrates, the PeLED area is 1 mm x 2 mm (Scale bar: 1 cm) and the driving voltage is 5 V.

VII. CONCLUSION

In this work, flexible PeLEDs are presented. A low-cost and room temperature manufacturing process is developed to

This article has been accepted for publication in a future issue of this journal, but has not been fully edited. Content may change prior to final publication. Citation information: DOI 10.1109/JEDS.2019.2913765, IEEE Journal of the Electron Devices Society

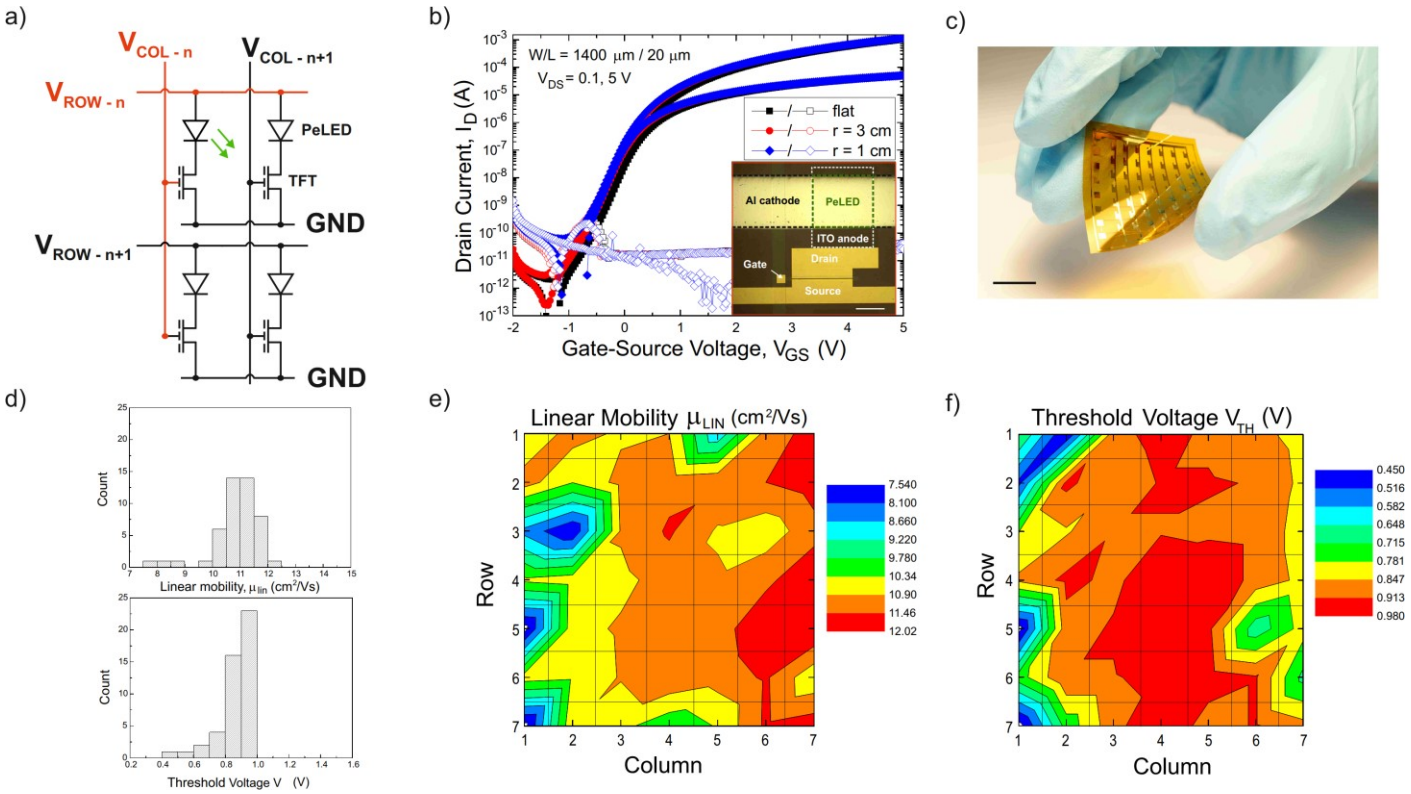

Fig. 5. Schematic and performance of the IGZO based active matrix. a) The green PeLED functionality is activated when the corresponding TFT is on-state (namely, its column and row lines are selected). The operating voltage for V_{COL} and V_{ROW} is 8 V. b) IGZO-based TFT characteristics (W/L = 1400 µm/20 µm) in flat and bent conditions. For each IGZO TFT, a PeLED is fabricated in series (inset) (Scale bar: 500 µm). c) The 7 x 7 active matrix is fabricated on a free-standing 50 µm thick kapton foil (Scale bar: 1 cm). The electrical performance of the matrix is evaluated. d) Histogram of the linear mobility μ_{lin} and threshold voltage V_{TH} for the array. Here, a yield of ≈ 96 % is achieved. e-f) Coloured 2D mapping of the same parameters over the substrate area (3 cm x 3 cm).

allow fabrication compatibility with flexible substrates. The green PeLEDs, realized on a 50 µm kapton foil with 2D $FAPbBr_3$ nanocrystals, show peak emission at 529 nm, turn-on voltage V_{on} of 2.8 V and a maximum current efficiency η_{CE} of 5.30 cd A^{-1}. To prove the device flexibility, dynamic bending experiments are performed, showing functionality while bent down to 10 mm bending radius for 5000 cycles. Moreover, passive matrixes as well as active arrays are realized on both rigid and flexible substrates, for the selective activation of multiple PeLEDs. Given the compatibility with standard IGZO TFT technology (room temperature and low-cost deposition), colloidal 2D $FAPbBr_3$ perovskites could represent a potential contestant for next-generation flexible display devices.

REFERENCES

[1] T. Someya, T. Sekitani, S. Iba, Y. Kato, H. Kawaguchi, and T. Sakurai, "A large-area, flexible pressure sensor matrix with organic field-effect transistors for artificial skin applications," *Proceedings of the National Academy of Sciences of the United States of America,* vol. 101, pp. 9966-9970, Jul 6 2004.

[2] T. Yokota, P. Zalar, M. Kaltenbrunner, H. Jinno, N. Matsuhisa, H. Kitanosako, *et al.*, "Ultraflexible organic photonic skin," *Science Advances,* vol. 2, Apr 2016.

[3] G. Cantarella, C. Vogt, R. Hopf, N. Munzenrieder, P. Andrianakis, L. Petti, *et al.*, "Buckled Thin-Film Transistors and Circuits on Soft Elastomers for Stretchable Electronics," *Acs Applied Materials & Interfaces,* vol. 9, pp. 28750-28757, Aug 30 2017.

[4] A. Koh, D. Kang, Y. Xue, S. Lee, R. M. Pielak, J. Kim, *et al.*, "A soft, wearable microfluidic device for the capture, storage, and colorimetric sensing of sweat," *Science Translational Medicine,* vol. 8, Nov 23 2016.

[5] Y. Chen, J. Au, P. Kazlas, A. Ritenour, H. Gates, and M. McCreary, "Electronic paper: Flexible active-matrix electronic ink display," *Nature,* vol. 423, p. 136, 2003.

[6] H. Sirringhaus, "25th Anniversary Article: Organic Field-Effect Transistors: The Path Beyond Amorphous Silicon," *Advanced Materials,* vol. 26, pp. 1319-1335, Mar 2014.

[7] M. K. Choi, J. Yang, K. Kang, D. C. Kim, C. Choi, C. Park, *et al.*, "Wearable red-green-blue quantum dot light-emitting diode array using high-resolution intaglio transfer printing," *Nature Communications,* vol. 6, May 2015.

[8] J. Jagielski, S. Kumar, W. Y. Yu, and C. J. Shih, "Layer-controlled two-dimensional perovskites: synthesis and optoelectronics," *Journal of Materials Chemistry C,* vol. 5, pp. 5610-5627, Jun 21 2017.

[9] S. Kumar, J. Jagielski, S. Yakunin, P. Rice, Y. C. Chiu, M. C. Wang, *et al.*, "Efficient Blue Electroluminescence Using Quantum-Confined Two-Dimensional Perovskites," *Acs Nano,* vol. 10, pp. 9720-9729, Oct 2016.

[10] S. Kumar, J. Jagielski, N. Kallikounis, Y. H. Kim, C. Wolf, F. Jenny, *et al.*, "Ultrapure Green Light-Emitting Diodes Using Two-Dimensional Formamidinium Perovskites: Achieving Recommendation 2020 Color Coordinates," *Nano Letters,* vol. 17, pp. 5277-5284, Sep 2017.

[11] J. Jagielski, S. Kumar, M. Wang, D. Scullion, R. Lawrence, Y.-T. Li*, et al.*, "Aggregation-induced emission in lamellar solids of colloidal perovskite quantum wells," *Science Advances,* vol. 3, p. eaaq0208, 2017.

[12] G. D. Niu, X. D. Guo, and L. D. Wang, "Review of recent progress in chemical stability of perovskite solar cells," *Journal of Materials Chemistry A,* vol. 3, pp. 8970-8980, 2015.

[13] L. Petti, N. Muenzenrieder, C. Vogt, H. Faber, L. Büthe, G. Cantarella*, et al.*, "Metal oxide semiconductor thin-film transistors for flexible electronics," *Applied Physics Reviews,* vol. 3, p. 021303, 2016.

[14] K. Nomura, H. Ohta, A. Takagi, T. Kamiya, M. Hirano, and H. Hosono, "Room-temperature fabrication of transparent flexible thin-film transistors using amorphous oxide semiconductors," *Nature,* vol. 432, p. 488, 2004.

[15] E. Fortunato, P. Barquinha, and R. Martins, "Oxide semiconductor thin‐film transistors: a review of recent advances," *Advanced materials,* vol. 24, pp. 2945-2986, 2012.

[16] G. Cantarella, V. Costanza, A. Ferrero, R. Hopf, C. Vogt, M. Varga*, et al.*, "Design of engineered elastomeric substrate for stretchable active devices and sensors," *Advanced Functional Materials,* p. 1705132, 2018.

[17] N. Münzenrieder, G. Cantarella, C. Vogt, L. Petti, L. Büthe, G. A. Salvatore*, et al.*, "Stretchable and conformable oxide thin‐film electronics," *Advanced Electronic Materials,* vol. 1, p. 1400038, 2015.